International Journal of Biochemistry and Cell Biology 112 (2019) 95–106

Contents lists available at ScienceDirect

International Journal of Biochemistry and Cell Biology

journal homepage: www.elsevier.com/locate/biocel

GPER1 influences cellular homeostasis and cytostatic drug resistance via influencing long chain ceramide synthesis in breast cancer cells

Marthe-Susanna Wegner[a,*,1], Lisa Gruber[a,1], Nina Schömel[a], Sandra Trautmann[a], Sebastian Brachtendorf[a], Dominik Fuhrmann[b], Yannick Schreiber[c], Catherine Olesch[b], Bernhard Brüne[b], Gerd Geisslinger[a,c], Sabine Grösch[a]

[a] pharmazentrum frankfurt/ZAFES, Institute of Clinical Pharmacology, Johann Wolfgang Goethe University, Theodor Stern-Kai 7, 60590 Frankfurt am Main, Germany
[b] Faculty of Medicine, Institute of Biochemistry I, Johann Wolfgang Goethe University, Theodor Stern-Kai 7, 60590 Frankfurt am Main, Germany
[c] Fraunhofer Institute for Molecular Biology and Applied Ecology IME, Project Group Translational Medicine and Pharmacology (TMP), Theodor Stern-Kai 7, 60590 Frankfurt am Main, Germany

ARTICLE INFO

Keywords:
Sphingolipids
Cell cycle progression
Autophagy
Mitochondrial stress
Glycolysis

ABSTRACT

The *G protein-coupled estrogen receptor 1* (GPER1) is involved in the regulation of physiological processes such as cellular growth and proliferation, but also in pathophysiological processes such as tumor development. The role of GPER1 in breast cancer is contradictory. Therefore, we investigated the influence of GPER1 overexpression on cellular processes in MCF-7 breast cancer cells. GPER1 overexpression leads to a cell cycle arrest in the G1 phase, induction of autophagy and reduced proliferation. Reduced proliferation was accompanied by a reduced basal respiration and reduced glycolysis rate in GPER1 overexpressing cells. This is presumably ascribable to mitophagy induction following GPER1 overexpression. However, GPER1 overexpressing cells were less sensitive against doxorubicin as compared to control cells. In previous work we showed the effect of transient GPER1 overexpression on the synthesis of several *ceramide synthases* (CerS) thereby influencing the sphingolipid pathway. Therefore, we investigated CerS expression and sphingolipid level in stable GPER1 overexpressing and control cells. Stable GPER1 overexpression strongly reduced CerS4, CerS5 and CerS6 promoter activity and CerS5 and CerS6 mRNA expression, whereas CerS2 mRNA expression was upregulated. The GPER1 effect on CerS5 promoter is mediated by GSK-3β signaling. In addition, other enzymes of the sphingolipid pathway were upregulated. Our study provides new insights into the role of GPER1 and the activated sphingolipid pathways and how GPER1 may influence cellular processes such as cancer cell survival following chemotherapy. Further studies are needed to investigate the molecular mechanisms leading to these cellular effects. Finding new therapeutic targets for modulating specifically GPER1 in breast tumors may improve endocrine breast cancer therapy.

1. Introduction

In woman, breast cancer is the second leading cause of cancer death in industrial countries (Ferlay et al., 2015). Despite early diagnosis and therapy strategies selected by hormone receptor status breast cancer leads to approximately 522.000 death cases per year (Ferlay et al., 2015). Reasons are the unknown molecular mechanisms, which provoke tumor genesis, tumor development and multidrug resistance during therapy. Identifying the precise molecular signaling pathways underlying for example tumor genesis are major goals in research to achieve an efficient and individual breast cancer therapy. 70–78 % of breast tumors exhibit a positive estrogen receptor (ER) status (Pujol et al., 1994; Chu and Anderson, 2002) meaning a higher expression level of the transcriptional more active ER subtype α as compared to expression of ERβ. ER positive tumors are declared to be hormone-responsive and therapy strategy is based either on lowering the estrogen level of the patients for example by aromatase blockage or by inhibiting the estrogen signaling by *selective ER modulators* (SERMs) such as tamoxifen or *selective ER downregulator* (SERD) such as fulvestrant (ICI 182,780).

* Corresponding author at: pharmazentrum frankfurt/ZAFES Johann Wolfgang Goethe University Institute of Clinical Pharmacology, House 74 Theodor Stern-Kai 7, 60590 Frankfurt am Main, Germany.
E-mail address: wegner@med.uni-frankfurt.de (M.-S. Wegner).
[1] Authors contributed equally to this work.

https://doi.org/10.1016/j.biocel.2019.05.002
Received 5 February 2019; Received in revised form 23 April 2019; Accepted 3 May 2019
Available online 11 May 2019
1357-2725/

In 1997, an orphan seven transmembrane-domain *G protein-coupled receptor 1* (GPER1 or also termed GPR30) with high affinity to 17β-estradiol (E2) was identified (Carmeci et al., 1997). GPER1 plays an important role in the regulation of physiological processes such as cellular growth and proliferation, but is also associated with pathophysiological processes such as tumor development (reviewed in (Olde and Leeb-Lundberg, 2009; Wang et al., 2010)). Beside E2 also other ER modulators such as *4-hydroxytamoxifen* (4-OHT), fulvestrant (Vivacqua et al., 2012) and bisphenol A (BPA) (Pupo et al., 2012) can bind to GPER1. Overexpression of GPER1 was positively associated with breast tumor size and the presence of metastases (Filardo et al., 2008) indicating poor prognosis for these patients and evidence emerged that targeting GPER1 would be beneficial for breast cancer therapy. It is shown that treatment of breast cancer with 4-OHT or fulvestrant can lead to multidrug resistance (Ignatov et al., 2010; Ignatov et al., 2011; Giessrigl et al., 2013). GPER1 resides in membrane structures and is responsible on the one hand for the rapid non-genomic actions of estrogen by activating protein kinase cascades and on the other hand for genomic alterations meaning altered gene transcription (reviewed in (Prossnitz et al., 2008; Wang et al., 2010)). GPER1 couples to the G proteins $G\alpha_s$, $G\alpha_{i/0,}$ and also to the Gβγ subunit thereby activating either *phospholipase C* (PLC) (Ca^{2+}) and *adenylate cyclase* (AC) or inhibiting AC activity leading to a decrease of *cyclic adenosine monophosphate* (cAMP) concentration (reviewed in (Nilsson et al., 2011; Wang et al., 2010)). Coupling to the Gβγ subunit activates the tyrosine-kinase Src, leading to release of *heparin-bound epidermal growth factor* (HB-EGF) and thereby transactivating the *epidermal growth factor receptor* (EGF-R). Subsequently, the *extracellular signal regulated kinase* (ERK) and *phosphoinositide 3 kinase* (PI3K)-AKT signaling pathways are induced (reviewed in (Nilsson et al., 2011)). This shows the complexity of the GPER1 signaling pathway. In addition, the function of GPER1 seems to vary between cancer types. Activated GPER1 induces c-Fos expression and proliferation in SKBr3 cells (ER -) (Maggiolini et al., 2004), but inhibits growth of ER + breast cancer cells (Ariazi et al., 2010). This shows that the function of GPER1 depends on the ER status of the cells and must be individually examined for each type of cancer cell line.

In previous work, we showed an upregulation of *ceramide synthases* (CerS) in breast cancer cells by estrogen (Wegner et al., 2014). CerS are key enzymes in the sphingolipid pathway and are important for cell proliferation. CerS are responsible for the production of ceramide, which is involved in physiological and pathophysiological processes such as apoptosis or autophagy following stress stimuli (reviewed in (Wegner et al., 2016), (Yamane et al., 2011; Fitzgerald et al., 2015; Brachtendorf et al., 2018)). Previously, we observed a GPER1-dependent transcriptional regulation of CerS (Wegner et al., 2014). This effect is estrogen-independently induced and is mediated by a transcription factor complex consisting of c-Fos and Fra-1 at the AP-1 binding site of the CerS promoter.

Here, we investigated the cellular effects of long term GPER1 overexpression. Our data indicate that GPER1 overexpressing cells (MCF-7/GPER1) exhibit a reduced cell cycle progression, enhanced autophagy and reduced ability for energy production. In addition, MCF-7/GPER1 cells are less sensitive against doxorubicin treatment, but more sensitive to the short-term cytotoxic effect of cyclophosphamide as compared to control cells. Fulvestrant treatment enhanced the cytotoxic effect of both substances in GPER1 overexpressing cells. Our study provides new insights into the cellular effects of GPER1 on breast cancer cell physiology and survival after chemotherapy.

2. Material and methods

2.1. Cell culture and treatment

The human breast adenocarcinoma cell line MCF-7 was purchased from the Health Protection Agency (European Collection of Cell Cultures, ECACC, Salisbury, UK) and was cultured in phenol-red free Dulbecco's Modified Eagle's Medium (DMEM) containing 4.5 g/L D-glucose, 5% charcoaled fetal bovine serum (FBS), 100 U/ml penicillin G and 100 µg/ml streptomycin, 5 mM sodium pyruvate and 1% GlutaMAX. G418-resistant cell selection was performed for 6 weeks and G418 sulfate was added in the culture media in a concentration of 200 µg/ml. Cells were incubated at 37 °C, in an atmosphere containing 5% CO_2. Fulvestrant was purchased from Sigma-Aldrich Laborchemikalien GmbH (Steinheim, Germany) and used in a concentration of 20 nM. Tocris Bioscience (Minneapolis, USA) provided the GPER1 agonist G1 ((±)-1-[(3aR*,4S*,9bS*)-4-(6-Bromo-1,3-benzodioxol-5-yl)-3a,4,5,9b-tetrahydro-3H-cyclopenta[c]quinolin-8-yl]-ethanone) (1 µM) and the GPER1 antagonist G15 ((3aS*,4R*,9bR*)-4-(6-Bromo-1,3-benzodioxol-5-yl)-3a,4,5,9b-3H cyclopenta[*c*]quinoline) (2.5 µM). Chloroquine (Merck, Darmstadt, Germany) was applied at 20 µM. The GSK-3β inhibitor SB-216763 (Santa Cruz Biotechnology, Dallas, Texas, USA) was added to transfected cells for luciferase reporter gene assay for 16 h at 10 µM.

2.2. Plasmid constructs and stable transfection

The GPER1 expression plasmid (GPER1-cDNA-pcDNA3.1) was purchased from cDNA Resource Center (Missouri University of Science & Technology, Rolla, USA) and the pTarget empty vector was purchased from OriGene Technologies Inc. (Rockville, USA). Plasmids were transfected using Lipofectamine® 2000 Reagent (Invitrogen, Thermo Fisher Scientific, Inc., Waltham, Massachusetts, USA) according to the manufacturer's protocol.

2.3. Immunocytochemistry

MCF-7/naiv, MCF-7/pTarget, and MCF-7/GPER1 cells were fixed in 4% paraformaldehyde, blocked with 5% Odyssey® Blocking Buffer (LI-COR Biotechnology, Lincoln, NE, USA), and incubated over night with anti-GPER1 and anti-PDI (Abcam, Cambridge, UK) primary antibody. Subsequently, cells were incubated with fragment cy3- (Sigma-Aldrich, St. Louis, Missouri, USA) and Alexa Fluor® 488- (Life Technologies, Carlsbad, CA, USA) conjugated secondary antibodies and examined with an Axio Observer Z1 microscope (Carl Zeiss AG, Oberkochen, Germany).

2.4. Cell size determination

Transmitted light image acquisition was used to determine the cell size by measuring the horizontal and vertical length of the cell by AxioVision software (Carl Zeiss AG, Oberkochen, Germany). Fifteen cells per cell line were analyzed and repeated at eight different cell passages.

2.5. cAMP level determination

MCF-7/pTarget and MCF-7/GPER1 were seeded at a density of 15.000 cells/well. After 16 h cells were harvested in 100 µl methanol. cAMP was isolated by methanol-extraction and determined by liquid chromatography tandem mass spectrometry using an Atlantis T3 column (100 mm x 2.1 mm I.D., 3 µm particle size; Waters, Eschborn, Germany).

2.6. Colony forming assay

Colony Forming Assay was performed to determine the effect of cyclophosphamide (CP) and doxorubicin (Doxo) on the proliferation of MCF-7/pTarget and MCF-7/GPER1 cells. Cells were treated with 10 µM CP and 20 nM Doxo and cultured for 10 days at 37 °C and 5% CO_2. Colonies were stained using 0.05% (w/v) crystal violet and the number of the colonies was calculated by ImageJ (National Institutes of Health, Bethesda, MD).

2.7. Cell viability assay

MCF-7/pTarget and MCF-7/GPER1 cells were seeded in 96-well plates at a density of 1×10^4 cells/well and treated with 0, 0.5, 1, 2, 5 and 9 μM Doxo and with 0, 80, 500, 1000, 2000 μM CP for 48 h. *Water soluble tetrazolium* (WST)-1 reagent (Roche Diagnostics, Rotkreuz, Switzerland) was added 1:10 (v/v). After 60 min incubation at 37 °C, absorbance was measured by Infinity® 200 PRO reader (Tecan Group, Männedorf, Switzerland) at a wavelength of 450 nm and 620 nm as reference.

2.8. Analysis of mitochondrial respiration and glycolysis

Oxygen consumption rate (OCR) and *extracellular acidification rate* (ECAR) in MCF-7/pTarget and MCF-7/GPER1 cells were analyzed using the Seahorse XFe Analyzer (Agilent, Technologies, Santa Clara, USA). Briefly, 1×10^4 cells/well were seeded in Seahorse 96-well cell culture plates. 1 h before the measurement cells were equilibrated in Krebs Henseleit buffer (111 mM NaCl, 4.7 mM KCl, 1.25 mM $CaCl_2$, 2 mM $MgSO_4$, 1.2 mM Na_2HPO_4) supplemented with 25 mM L-glucose and 3 mM L-glutamine. To block ATP-coupled respiration 2.5 μM oligomycin (Sigma-Aldrich, St. Louis, Missouri, USA) was added. Cells were treated with 1 μM carbonyl cyanide m-chlorophenylhydrazone (CCCP) (Sigma-Aldrich, St. Louis, Missouri, USA) to uncouple the respiratory chain and 1 μM rotenone (Sigma-Aldrich, St. Louis, Missouri, USA) and 1 μg/ml antimycin A (Sigma-Aldrich, St. Louis, Missouri, USA) to block mitochondrial respiration.

2.9. Quantitative real-time-PCR

Total RNA was isolated using RNeasy Mini Kit (Qiagen, Venlo, Netherlands). cDNA was synthesized from 300 ng total RNA using VERSO™ cDNA Kit (Thermo Fisher, ABgene, Epsom, UK). Gene-specific PCR products were assayed using Maxima Evergreen qPCR Master Mix on a 7500fast quantitative PCR system (TaqMan®, Life Technologies, Darmstadt, Germany). Relative gene expression was determined using the comparative cycle threshold method, normalizing relative values to the expression level of RPL37A as a housekeeping gene. The primer mixes of nSMase1, 2 and 3 were purchased from GeneCopeia (Rockville, USA) and the GPER1-primermix from Realtimeprimers (Elkins Park, Philadelphia, USA) (Table 1). Primer for RPL37A, CerSX, SPHK1, CERK, ASAH1, aSMase, MFN1 and 2, Parkin, Fis1 and PINK were purchased from Eurofins Genomics (Ebersberg, Germany).

2.10. Western blot analysis

For protein analysis by western blot, total protein was isolated. Cells were harvested and resuspended in PhosphoSafe™ buffer (EMD Chemicals, Inc. La Jolla, USA), 2 mM DTT (AppliChem GmbH, Darmstadt, Germany), 1x Roche Complete (Roche, Mannheim, Germany), pH 7.4. The solution was sonicated and centrifuged (14,000 x g, 10 min, 4 °C). For determination of total protein concentration the Bradford method was used. 60 μg proteins was separated electrophoretically by 12% SDS-PAGE and then transferred onto nitrocellulose membranes and blocked for 90 min at room temperature in Odyssey blocking reagent (LI-COR Biosciences, Bad Homburg, Germany) diluted 1:1 in PBS. Membranes were incubated overnight at 4 °C with primary antibody against GPER1 (rabbit) (Abcam, Cambridge, UK), HA-Tag (Abcam, Cambridge, UK), p62 (mouse) (Abcam, Cambridge, UK) or LC3B (rabbit) (Cell Signaling Technology, Danvers, Massachusetts, USA) and Hsp90 (BD, Franklin Lakes, New Jersey, USA) was used as loading control. Densitometric analysis of the Blots was performed with Image Lite Software (LI-COR, Biosciences, Lincoln, USA).

2.11. Determination of sphingolipid concentrations by high performance liquid chromatography tandem mass spectrometry

Sphingolipid concentrations were quantified by liquid chromatography coupled to tandem mass spectrometry (LC–MS/MS) as described previously (Wegner et al., 2014).

2.12. Proliferation assay

For quantitative proliferation assays, cells were seeded at a density of 5×10^4 cells/dish. After stimulation, cells were harvested at day 1, day 2, day 3 and day 4 and the number of living cells was counted using a Neubauer counting chamber (LO-Laboroptik, Bad Homburg, Germany).

2.13. Cell cycle analysis

Cell cycle distribution was evaluated by flow cytometry using propidium iodide (PI, Sigma, Darmstadt, Germany) staining on a flow cytometer (FACSCanto II, BectonDickinson, Heidelberg, Germany). Cells were starved for 24 h with 1% FCS and treated for 24 h. They were harvested by trypsin, washed with 1 x PBS and fixed with 80% (v/v) ethanol overnight at −20 °C. After two washing steps with 1 x PBS, cells were incubated for 5 min with 0.125% Triton X-100 on ice,

Table 1
Oligonucleotide sequences for RT-PCR.

Gene	Sequence (5`→3`)			
	Forward primer	Reverse primer	T [° C]	Amplicon size [bp]
RPL37A	ATT GAA ATC AGC CAG CAC GC	AGG AAC CAC AGT GCC AGA TCC	60	94
CerS2	CCA GGT AGA GCG TTG GTT	CCA GGG TTT ATC CAC AAT GAC	57	141
CerS4	CTG GTG GTA CCT CTT GGA GC	CGT CGC ACA CTT GCT GAT AC	60	105
CerS5	CAA GTA TCA GCG GCT CTG T	ATT ATC TCC CAA CTC TCA AAG A	57	122
CerS6	AAG CAA CTG CAG TGG GAT GTT	AAT CTG ACT CCG TAG GTA AAT ACA	60	145
SPHK1	GTC ACG TGC AGC CCC TTT	CGC GCG TGG TTC CG	60	76
CERK	TAA CCC CCA AAG TCA CAA AA	CAT CTC CAC CAA CAC AGA CA	57	182
ASAH1	TGT GGA TAG GGT TCC TCA CTA GA	TTG TGT ATA CGG TCA GCT TGT TG	60	375
aSMase	CCT GGA GAG CCT GTT GAG TG	GTT GGT CCT GAC GAG TCT GG	60	110
nSMase1	CAT GGT GAC TGG TTC AGT GG	TAG AGC TGG GGT TCT GCT GT	60	553
nSMase2	CAA CAA GTG TAA CGA CGA TGC C	CGA TTC TTT GGT CCT GAG GTG T	60	89
nSMase3	CAC CCA GGA TGA GAA TGG AAA	GTC CGT CCT CAC CCA CGA T	60	59
MFN1	ATGACCTGGTGTTAGTAGACAGT	AGACATCAGCATCTAGGCAAAAC	60	90
MFN2	CACATGGAGCGTTGTACCAG	TTGAGCACCTCCTTAGCAGAC	60	104
Parkin	GTGTTTGTCAGGTTCAACTCCA	GAAAATCACACGCAACTGGTC	60	129
FIS1	GATGACATCCGTAAAGGCATCG	AGAAGACGTAATCCCGCTGTT	60	82
PINK	CCCAAGCAACTAGCCCCTC	GGCAGCACATCAGGGTAGTC	60	107

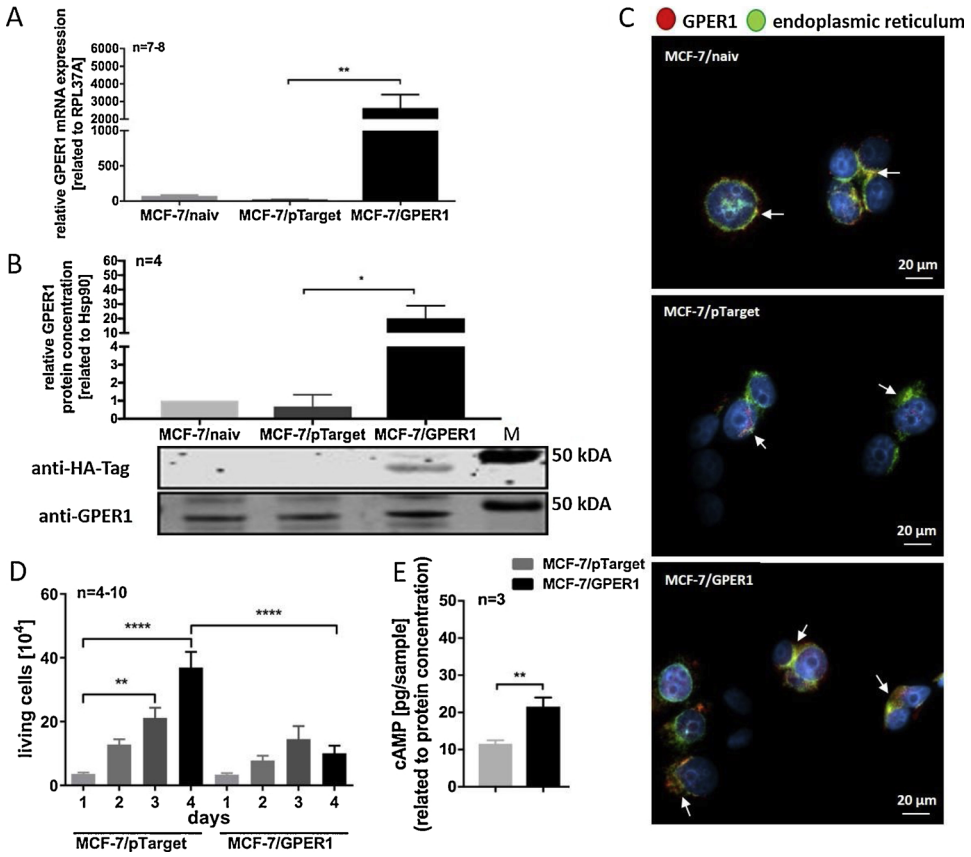

Fig. 1. Validation of GPER1 overexpression in MCF-7 cells. (A) GPER1 mRNA expression determination by qRT-PCR. The mRNA expression is related to the housekeeping gene RPL37A. Data are presented as a mean of n = 7–8 ± SEM (standard error of the mean). Unpaired *t* test with Welch's correction. (B) GPER1 protein concentration determination by Western blot analysis. An anti-HA-Tag antibody was used to detect protein resulting from stable transfection and an anti-GPER1 antibody was used to detect endogenous GPER1 protein. Data are represented as a mean of n = 4 ± SEM (standard error of the mean). Unpaired *t* test with Welch's correction. (**C**) Immunocytochemistry of MCF-7 cells. Cells were incubated with an anti-GPER1 and anti-PDI (endoplasmic reticulum) antibody and subsequently incubated with secondary antibodies. DAPI (4′,6-diamidino-2-phenylindole) was used to stain DNA. Images were recorded by Axio Observer. Z1 microscope (Carl Zeiss AG, Oberkochen, Germany). (D) Living cell number determination by Neubauer counting chamber on day 1–4. Data are represented as a mean of n = 3 ± SEM (standard error of the mean). Unpaired *t* test with Welch's correction. (E) Determination of cAMP levels in MCF-7cells by LC–MS/MS. Data are represented as a mean of n = 3 ± SEM (standard error of the mean). Unpaired *t* test with Welch's correction. M = Marker. $*p \leq 0.05$, $**p \leq 0.01$, $****p \leq 0.0001$.

washed again with 1 x PBS and then stained with PI (20 µg/ml) (Sigma, Darmstadt, Germany) in 1 x PBS containing 0.2 mg/ml RNaseA (Qiagen, Hilden, Germany). 100.000 cells were analyzed per sample. G1, S and G2/M fractions were quantified using FlowJo (FlowJo, LLC, Ashland, Oregon) and manual gating.

2.14. Promoter reporter gene assay

Cells were seeded at 2×10^4/96-well plate and transfection was performed with Lipofectamine® 2000 Reagent (Invitrogen by Life Technologies, Carlsbad, USA) according to the manufacturer's protocol. They were transfected with 200 ng of the distinct Firefly luciferase reporter vector (pRL-TK, Promega, Fitchburg, USA), with GPER1-cDNA-pcDNA3.1 construct, CerS2, CerS4, CerS5 and CerS6 constructs. Next steps were performed as described previously (Wegner et al., 2014).

2.15. Detection of intracellular-induced signaling pathways

For analysis of signaling pathways in MCF-7 cells, the Pathscan® Intracellular Signaling Array Kit (Cell Signaling, Cambridge, UK) was used. This antibody array detects several phosphorylated signaling proteins. The assay was performed according to the manufacturer's protocol.

2.16. Statistical analysis

Data are presented as mean ± SEM (standard error of the mean). Statistical analyses were performed with the GraphPad Prism 7 software (GraphPad Software, San Diego, CA, USA). Outliers wer detected by ROUT analysis. Significant differences between groups were assessed by using the Unpaired *t* test with Welch's correction (two-tailed test).

3. Results

3.1. Stable transfection of the GPER1 expression plasmid

We generated stably GPER1 overexpressing MCF-7 cells (MCF-7/GPER1) and control cells (MCF-7/pTarget = empty vector; MCF-7/naiv = untransfected cells). The mRNA concentration of GPER1 is significantly induced in MCF-7/GPER1 cells as compared to control cells (Fig. 1A), which is verified on protein level (Fig. 1B). For overexpression analysis, HA-Tag detection was performed and for detection of endogenous GPER1 protein, an anti-GPER1 antibody was used. GPER1 localizes in the endoplasmic reticulum, but also exhibits a perinuclear localization, which is unknown (Fig. 1C and supporting information 1B). In addition, cell proliferation is inhibited (Fig. 1D) and intracellular cAMP concentration is increased in MCF-7/GPER1 cells as compared to control cells (Fig. 1E), which is in line with previously published data, showing that GPER1 inhibits cells growth of ER + cells

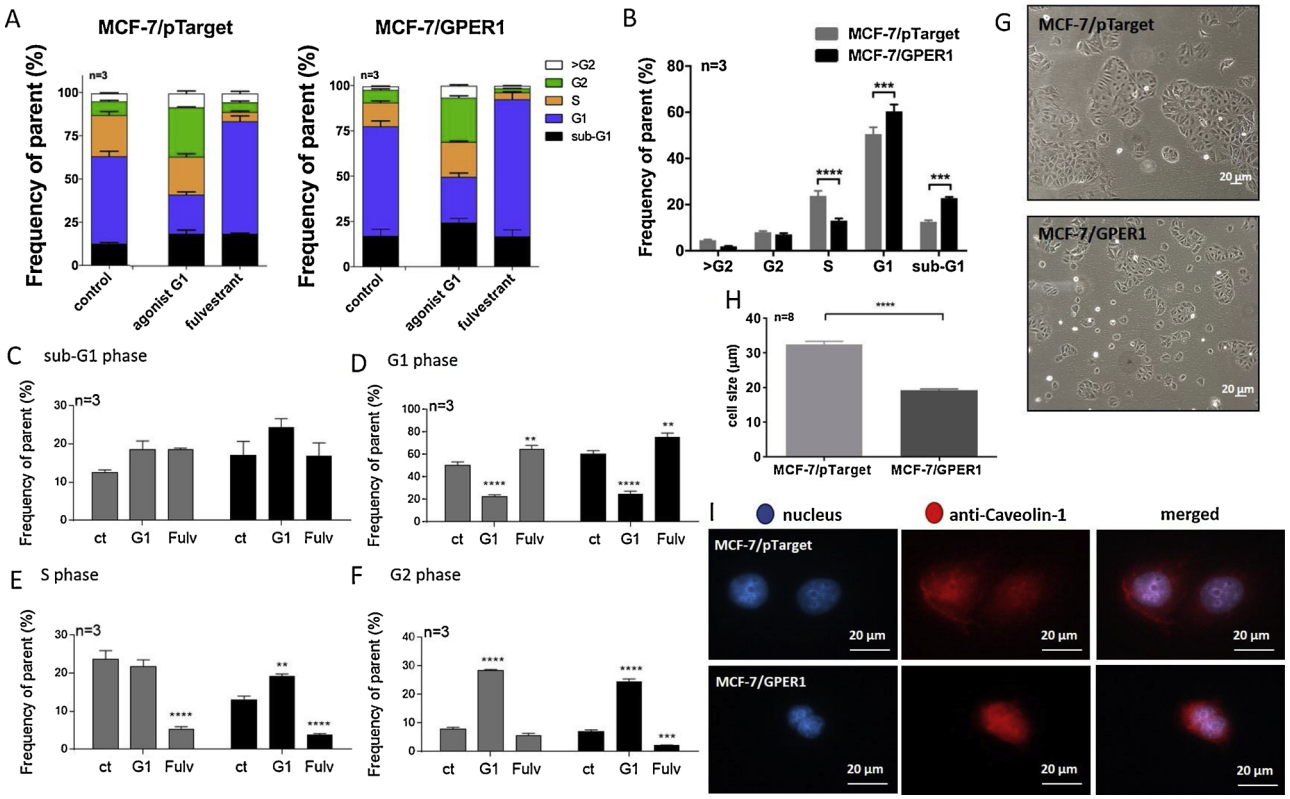

Fig. 2. Impact of a GPER1 overexpression on cell cycle progression. (A) Summary of the flow cytometry analysis following G1 and fulvestrant stimulation. Data are represented as a mean of n = 3 ± SEM (standard error of the mean). Unpaired *t* test with Welch's correction. (B) Flow cytometry analysis of MCF-7/GPER1 and control cells. Data are represented as a mean of n = 3 ± SEM (standard error of the mean). Unpaired *t* test with Welch's correction. (C) Frequency of parent (%) in the sub-G1 phase following G1 and fulvestrant stimulation. Data are represented as a mean of n = 3 ± SEM (standard error of the mean). Unpaired *t* test with Welch's correction. (**D**) Frequency of parent (%) in the G1 phase following G1 and fulvestrant stimulation. Data are represented as a mean of n = 3 ± SEM (standard error of the mean). Unpaired *t* test with Welch's correction. (E) Frequency of parent (%) in the S phase following G1 and fulvestrant stimulation. Data are represented as a mean of n = 3 ± SEM (standard error of the mean). (F) Frequency of parent (%) in the G2 phase following G1 and fulvestrant stimulation. Data are represented as a mean of n = 3 ± SEM (standard error of the mean). Unpaired *t* test with Welch's correction (G) Transmitted light image acquisition shows a decreased cell size of MCF-7/GPER1 cells compared to control cells. (H) Cell size determination. Data are represented as a mean of n= ± SEM (standard error of the mean). Unpaired *t* test with Welch's correction. (**I**) Immunocytochemistry of MCF-7 cells. Cells were incubated with an anti-caveolin-1 antibody and subsequently incubated with secondary antibodies. DAPI (4′,6-diamidino-2-phenylindole) was used to stain DNA. Images were recorded by Axio Observer. Z1 microscope (Carl Zeiss AG, Oberkochen, Germany). $^{**}p \leq 0.01$, $^{***}p \leq 0.001$, $^{****}p \leq 0.0001$.

(Ariazi et al., 2010), and verifies the functionality of overexpressed GPER1. In summary, overexpression of GPER1 in MCF-7 cells is verified and associated with higher cAMP level and reduced cell proliferation.

3.2. GPER1 overexpression inhibits cell cycle progression

To investigate how GPER1 overexpressing leads to an inhibition of cell proliferation (Fig. 1D) we analyzed cell cycle progression by flow cytometry. MCF-7/GPER1 cells accumulate in the G1 and sub-G1 cell cycle phase, which is accompanied by a decrease of number of cells in the S phase as compared to control cells (Fig. 2A and B). MCF-7/GPER1 cells also show a reduced cell size phenotype (Fig. 2G and H). Both nucleus and the surrounding cell parts of MCF-7/GPER1 cells are reduced in size as compared to control cells (Fig. 2I), whereas flow cytometry analysis shows no differences (supporting information 2). The GPER1 agonist G1 arrests MCF-7/GPER1 and control cells in the G2/M phase (Fig. 2F), which indicates that the GPER1 agonist G1 effect is GPER1 independent. Fulvestrant leads to a significant increase of cells in the G1 phase, which is more pronounced in MCF-7/GPER1 cells (Fig. 2D). This is accompanied by a reduced frequency of cells in the S and G2/M phase in MCF-7/GPER1 and control cells (Fig. 2E and F). In summary, overexpression of GPER1 negatively regulates cell cycle progression by blocking cells in the G1 phase and combination of GPER1 overexpression and fulvestrant treatment amplifies the effect on cell cycle progression.

3.3. GPER1 overexpression influences cell energy production

Estrogens are important regulators of mitochondrial activity (Oo et al., 2018) and it has been shown that they act via binding and activating estrogen receptor subtypes α and β as well as by binding to GPER1 (Klinge, 2017). Therefore, we investigated the metabolic state of MCF-7/GPER1 and control cells. The basal *oxygen consumption rate* (OCR), which represents basal mitochondrial respiration is reduced in MCF-7/GPER1 cells as compared to control cells (Fig. 3A). The ATP-linked respiration (Oligomycin injection) is unaltered following GPER1 overexpression. *Carbonyl cyanide m-chlorophenylhydrazone* (CCCP) uncouples respiration from oxidative phosphorylation by decreasing mitochondrial membrane potential (ΔΨm). The maximal respiration rate and the reverse capacity, which can be deduced from values following CCCP injection, are enhanced in MCF-7/GPER1 cells as compared to control cells. The data indicate that GPER1 overexpressing cells have no general defect in the mitochondrial respiratory capacity, but lower basal OCR might be related to a reduced catabolic activity. In line with these findings we detected a clearly reduced *extracellular acidification rate* (ECAR) (measures the glycolysis rate of the cells) in MCF-7/GPER1 cells in comparison to MCF-7/pTarget cells (Fig. 3B). Under mitochondrial stress the ability to perform glycolysis is even more limited.

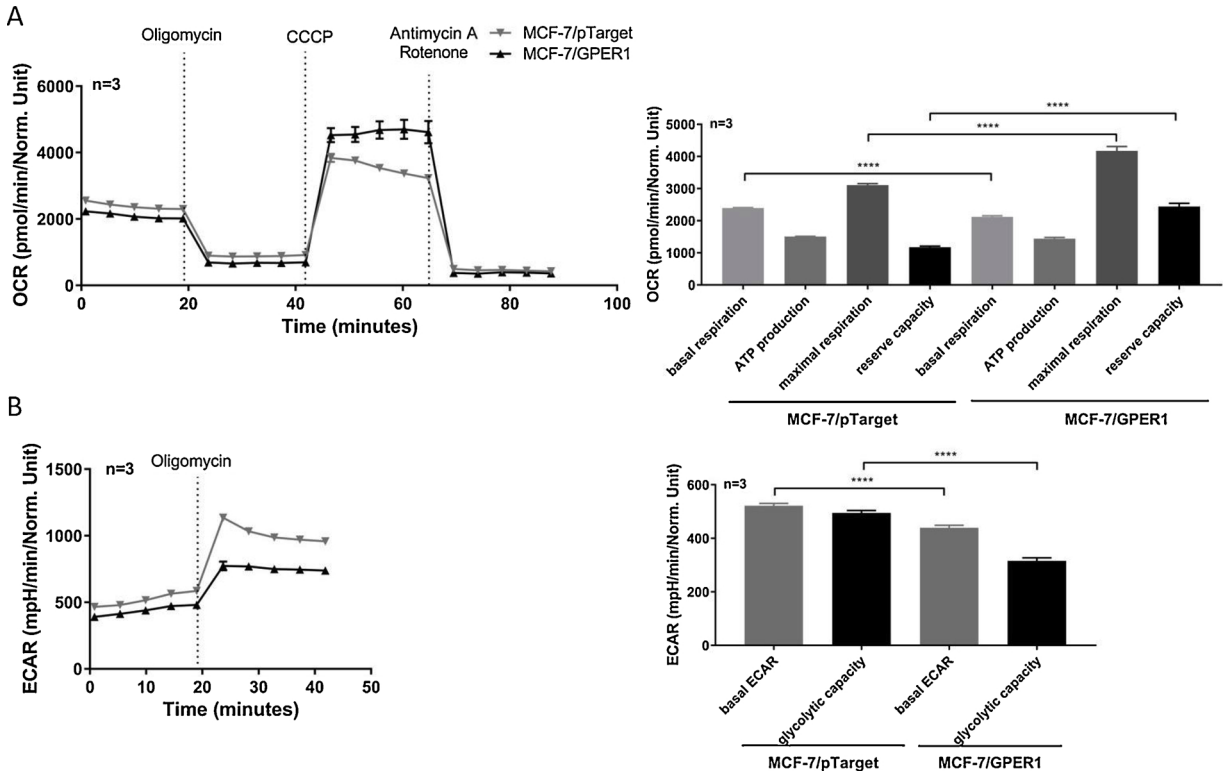

Fig. 3. GPER1 impact on energy metabolism. (A) *Oxygen consumption rate* (OCR) analyzed by Seahorse XF 96 analyzer. Data are represented as a mean of n = 3 ± SEM (standard error of the mean). Unpaired *t* test with Welch's correction. (B) *Extracellular acidification rate* (ECAR) analyzed by Seahorse XF 96 analyzer. ATP production and glycolytic capacity were derived by calculating the difference of the data before and after the addition of oligomycin. The maximal respiration is the difference of the rates after CCCP treatment and after antimycin A and rotenone treatment, whereas the reverse capacity is calculated by the difference of data after CCCP treatment and basal respiration. Data are represented as a mean of n = 3 ± SEM (standard error of the mean). $*p \leq 0.05$, $**p \leq 0.01$, $****p \leq 0.0001$.

The reduced catabolic activity might be related to the diminished proliferation rate of these cells, but future experiments will show if it is the cause or the consequence of the lower proliferation.

3.4. GPER1 overexpression induces autophagic processes

Since GPER1 overexpression influences cell cycle progression negatively we investigated the impact of GPER1 overexpression on autophagic processes. GPER1 overexpression leads to an increased light chain (LC)3B II/LC3B I ratio, which indicates autophagy induction in MCF-7/GPER1 cells as compared to control cells., This is also present when the autophagic flux is blocked with *chloroquine* (CQ) (Fig. 4A and supporting information 3A). Fulvestrant treatment leads to an even stronger induction of the LC3B II/LC3B I ratio, which indicates enhanced autophagy in MCF-7/GPER1 cells following fulvestrant stimulation (Fig. 4B). G1 stimulation induces a G2/M phase block (Fig. 2), but does not lead to autophagy induction (Fig. 4B). To verify the results, we also investigated p62 protein levels, which are significantly decreased in MCF-7/GPER1 cells following fulvestrant treatment as compared to control cells (Fig. 4C and supporting information 3B). p62 binds directly to LC3B and is degraded by autophagy. Therefore, the p62 level correlates negatively with the autophagic flux (Bjørkøy et al., 2005). In summary, MCF-7/GPER1 cells exhibit an augmentation of autophagic processes, which could be further enhanced by fulvestrant treatment.

3.5. GPER1 overexpression desensitizes cells growing in colonies against doxorubicin

The potential of GPER1 promoting cancer or exhibiting anti-carcinogenic effects is currently under debate. In our study GPER1 overexpression in MCF-7 cells leads to a reduced proliferation rate as compared to control cells (Fig. 1D). Accordingly, we were interested in the anti-carcinogenic effects of commonly used chemotherapeutics in our cell system. We investigated the influence of cyclophosphamide and doxorubicin stimulation on the ability of the cells to grow in colonies and the influence on the cell toxicity. Following 10 days of cultivation with cyclophosphamide or doxorubicin, the colony formation is significantly reduced in MCF-7/GPER1 and control cells (Fig. 5A and supporting information 4). Interestingly, MCF-7/GPER1 cells were significantly less sensitive against doxorubicin in comparison to control cells. This was not due to a direct protective effect of GPER1 against the cytotoxic effect of doxorubicin, because the WST assay (cell viability) shows no differences between MCF-7/GPER1 and control cells following doxorubicin stimulation for 48 h (Fig. 5B). Co-stimulation with fulvestrant sensitized both MCF-7/GPER1 and MCF-7/pTarget cells against the cytotoxic effect of doxorubicin (Fig. 5B). In contrast to the data of the colony forming assay, which shows no difference between MCF-7/GPER1 and control cells following cyclophosphamide treatment, MCF-7/GPER1 cells were clearly more sensitive against the cytotoxic effect of 48 h cyclophosphamide treatment, which could be further pronounced by fulvestrant co-treatment (Fig. 5B). These data indicate that overexpression of GPER1 in ER + breast cancer cells leads to diverse cellular effects following chemotherapy depending on the drug and the respective mode of action in the cell. Co-treatment with fulvestrant sensitizes GPER1 overexpressing cells to cytotoxic drugs.

3.6. GPER1 effect on sphingolipid level

Our data show that GPER1 overexpression is related to a reduced cell proliferation, cell cycle block, induction of autophagy and resistance to cytostatic drugs. Based on previous work we know that these processes are strongly influenced by sphingolipids and that especially ceramides may play an important role (Grösch et al., 2012). In previous

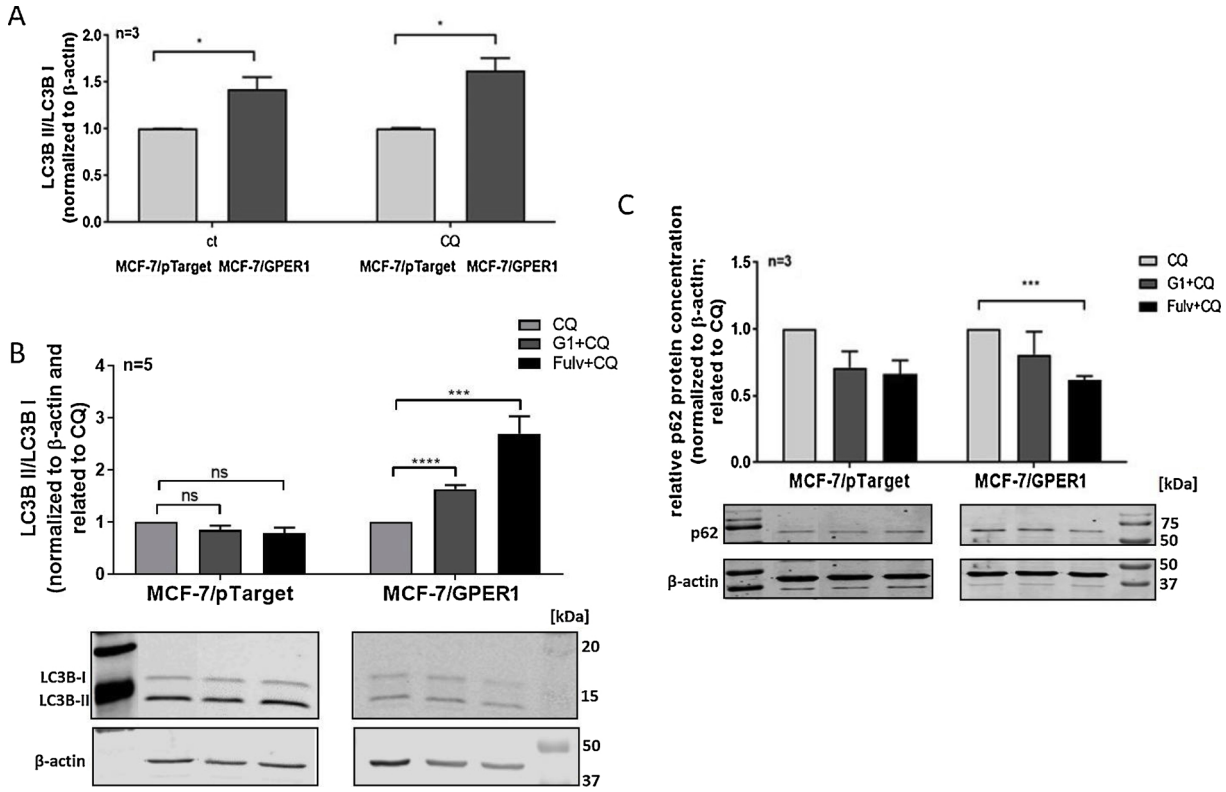

Fig. 4. GPER1 impact on autophagy induction. (A) Analysis of autophagic processes by determination of LC3B II/LC3B I ratio by Western blot analysis (control). Data are represented as a mean of n = 3 ± SEM (standard error of the mean). Unpaired *t* test with Welch's correction. (B) Analysis of autophagic processes by determination of LC3B II/LC3B I ratio by Western blot analysis (chloroquine = CQ). The protein expression is related to the housekeeping protein β-actin. Data are represented as a mean of n = 3 ± SEM (standard error of the mean). (**C**) Analysis of p62 protein levels by Western blot analysis. The protein expression is related to the housekeeping protein β-actin. Data are represented as a mean of n = 3 ± SEM (standard error of the mean). Unpaired *t* test with Welch's correction. Unpaired *t* test with Welch's correction. $^{*}p \leq 0.05$, $^{**}p \leq 0.01$, $^{***}p \leq 0.001$.

work we showed the effect of a transient GPER1 overexpression over a time period of 48 h on the expression of several ceramide synthases (CerS) in MCF-7 cells (Wegner et al., 2014). In this study, we investigated the promotor activity of CerS2, CerS4, CerS5 and CerS6 (the most abundant CerS in MCF-7 cells) in stably transfected MCF-7/GPER1 (permanent GPER1 overexpression) and MCF-7/pTarget cells. The promotor activities of CerS4, CerS5 and CerS6 were significantly downregulated in GPER1 overexpressing cells, whereas CerS2 promotor activity was not affected (Fig. 6A). However, the mRNA level analysis shows an increase of CerS2 and a decrease of CerS5 and CerS6 mRNA expression (Fig. 6B). The differences between CerS promoter activity and CerS mRNA expression could be due to post-transcriptional regulation such as binding of microRNAs at the respective mRNA (reviewed in (Wegner et al., 2016)). We also investigated the mRNA expression of other sphingolipid metabolizing enzymes. Acid ceramidase (ASAH1), acid sphingomyelinase (aSMase), neutral sphingomyelinase 1 (nSMase1), sphingomyelin synthase 1/2 (SMS1/2) and ceramide kinase (CERK) mRNA expression are increased in MCF-7/GPER1 cells (Fig. 6C and supporting information 5). Since the mRNA expression of enzymes involved in the catabolism and anabolism of sphingolipids increased in parallel, we examined the sphingolipid level in MCF-7/GPER1 and control cells. Almost all detected sphingolipids are decreased in MCF-7/GPER1 cells as compared to control cells (Fig. 6D). Sphingolipids are important compounds of cellular membranes, but also act as signaling molecules. Our data indicate that GPER1 overexpression in MCF-7 cells leads to an overall reduction of sphingolipids. However, further studies are needed to explain whether or not changes in the sphingolipid level are responsible for our observed cellular effects mediated by overexpression of GPER1. Since cell energy production is altered following GPER1 overexpression (Fig. 3), we analyzed mRNA expression of genes, which regulate autophagy and fusion/fission events in mitochondria. *Mitofusion 1* (MFN1) and *2* (MFN2) mRNA expression is significantly increased in MCF-7/GPER1 cells as compared to control cells, whereas *mitochondrial fission 1 protein* (FIS1) mRNA expression is decreased (Fig. 6D and supporting information 5). In addition, MCF-7/GPER1 cells exhibit an increased Parkin mRNA expression, whereas the *mitochondrial serine/threonine protein kinase* (PINK) is unaltered. These data indicate a shift from mitochondrial fission events to more fusion events in MCF-7/GPER1 cells as compared to control cells.

3.7. CerS5 promoter activity is GSK-3β mediated

To identify altered activity of signaling proteins following GPER1 overexpression we analyzed signaling pathways using the Pathscan® Intracellular Array Kit. The antibody-based analysis shows an increased phosphorylation of Akt473 and *glycogen synthase kinase-3β* (GSK-3β) in MCF-7/GPER1 cells as compared to control cells, whereas Akt308 phosphorylation is unaltered (Fig. 7A and B). To investigate whether or not activated GSK-3β mediates the inhibitory effect on CerS5 promoter activity following GPER1 overexpression, we analyzed CerS5 promoter activity following GSK-3β inhibition with SB-216763. Inhibition of GSK-3β leads to a significant increase in CerS5 promoter activity (Fig. 7C) indicating that activated GSK-3β mediates CerS5 promotor activity suppression.

4. Discussion

In the literature the role of GPER1 in breast cancer is controversially discussed. On the one hand it has been shown that GPER1 is associated with increased disease-free survival in ER + breast cancer patients

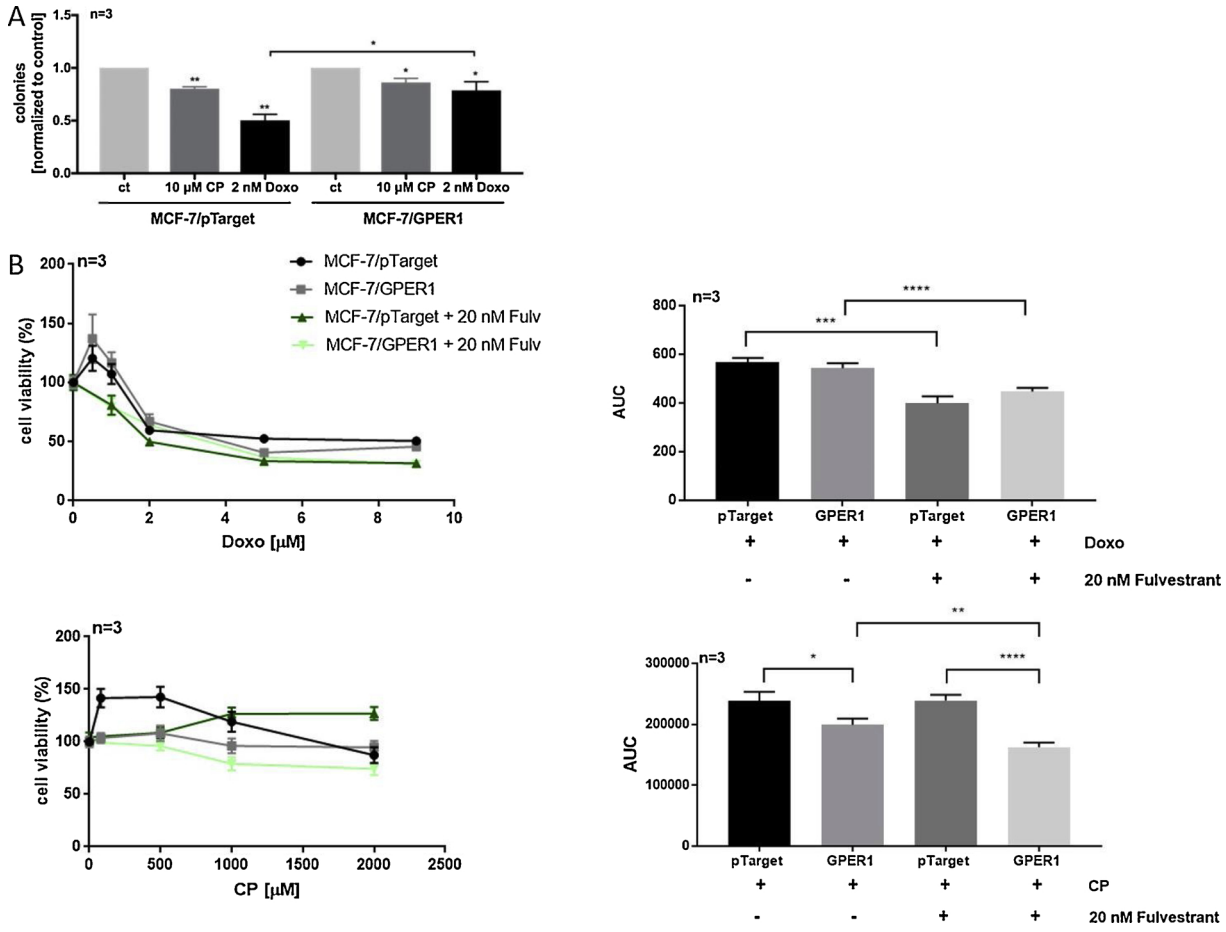

Fig. 5. GPER1 impact on colony forming and cell viability following cytostatic drug treatment. (A) Colony Forming Assay following cyclophosphamide (CP) and doxorubicin (Doxo) stimulation. Data are represented as a mean of n = 3 ± SEM (standard error of the mean). Unpaired *t* test with Welch's correction. (B) Cell viability analysis (WST assay) with and without 20 nM fulvestrant (Fulv) treatment. Area under curve = AUC. Data are represented as a mean of n = 3 ± SEM (standard error of the mean). Unpaired *t* test with Welch's correction. $^{*}p \leq 0.05$, $^{**}p \leq 0.01$, $^{****}p \leq 0.0001$.

(Broselid et al., 2013), but it is related to metastasis of ER- breast cancer cells (Jiang et al., 2013). GPER1 was also associated with opposite effects in HER2 positive (poor *disease-free survival* (DSF)) and HER2 negative (better DSF) breast cancer patients (Yang and Shao, 2016). Here, we investigated the effect of GPER1 overexpression on the ER +, but HER2 negative breast cancer cell line MCF-7. We were able to show that an increased GPER1 expression leads to inhibition of cell cycle progression, induction of autophagic processes, reduced mitochondrial activity and cytostatic drug resistance. We could also show that GPER1 overexpression negatively regulates CerS4, CerS5 and CerS6 promotor activity and decreases several sphingolipid specie levels in MCF-7 cells.

Our immunocytochemistry shows that GPER1 localizes in the endoplasmic reticulum, but also exhibits a perinuclear localization, which is unknown (Fig. 8). This localization might be lysosomes in which unfolded GPER1 protein is degraded. The physiological subcellular localization of GPER1 is currently under discussion. Revankar et al. showed that GPER1 resides in the endoplasmic reticulum by using fluorescent estrogen derivatives (Revankar, 2005). Recently, it could been shown that non-glycosylated GPER1 accumulates in the nucleus, thereby binding as a transcription factor-like molecule at the promoter of *c-Fos* and *connective tissue growth factor* (*CTGF*) and stimulates breast cancer cell migration (Pupo et al., 2017). Accordingly, GPER1 might localize in different cellular compartments, which is possibly dependent on posttranslational modifications of the protein. GPER1 overexpression also leads to a decreased cell size (Fig. 8).

It has been shown that GPER1 promotes *fibronectin* (FN) matrix assembly (Quinn et al., 2009) and formation of focal adhesions leading to the reorganization of actin stress fibers (Magruder et al., 2014). Altered expression of FN is associated with the development of cancer and integrin-based adhesion has served as a model for studying the central role of adhesion in migration, but FN alterations could also be involved in the adaption of cell size (reviewed in (Kang et al., 2015)).

GPER1 overexpression reduced cell proliferation and mitochondrial activity and induced autophagy in MCF-7 cells. Our data show that overexpression of GPER1 leads to an increase in cAMP concentration in MCF-7 cells as compared to control cells. cAMP is a known activator of PKA, which subsequently may lead to phosphorylation of *dynamin-related protein 1* (Drp1) (Fig. 8). Drp1 controls the life of a mitochondrion by mediating mitochondrial fission events, which lead to an increased mitochondrial number (reviewed in (Hu et al., 2017; Oo et al., 2018)). When Drp1 is phosphorylated less fission events occur, which shifts the fission/fusion balance towards fusion (Mozdy et al., 2000)An increase of fusion events means that the mitochondrial mass increases as well as cell protectiive events (reviewed in (Jahani-Asl and Slack, 2007)). The reduced FIS1 mRNA expression in MCF-7/GPER1 cells as compared to control cells confirms the reduced number of mitochondrial fission events following GPER1 overexpression. The process of mitochondrial fusion is stimulated by cellular stress (Youle and van der Bliek, 2012). We showed that GPER1 overexpression leads to cellular stress, which is also indicated by less execution of glycolysis and oxidative phosphorylation in MCF-7/GPER1 cells (Fig. 8). The question arises whether there is a link between induction of autophagy and reduced mitochondrial activity, the so-called mitophagy. The connection between GPER1 and mitochondrial activity was examined by different groups.

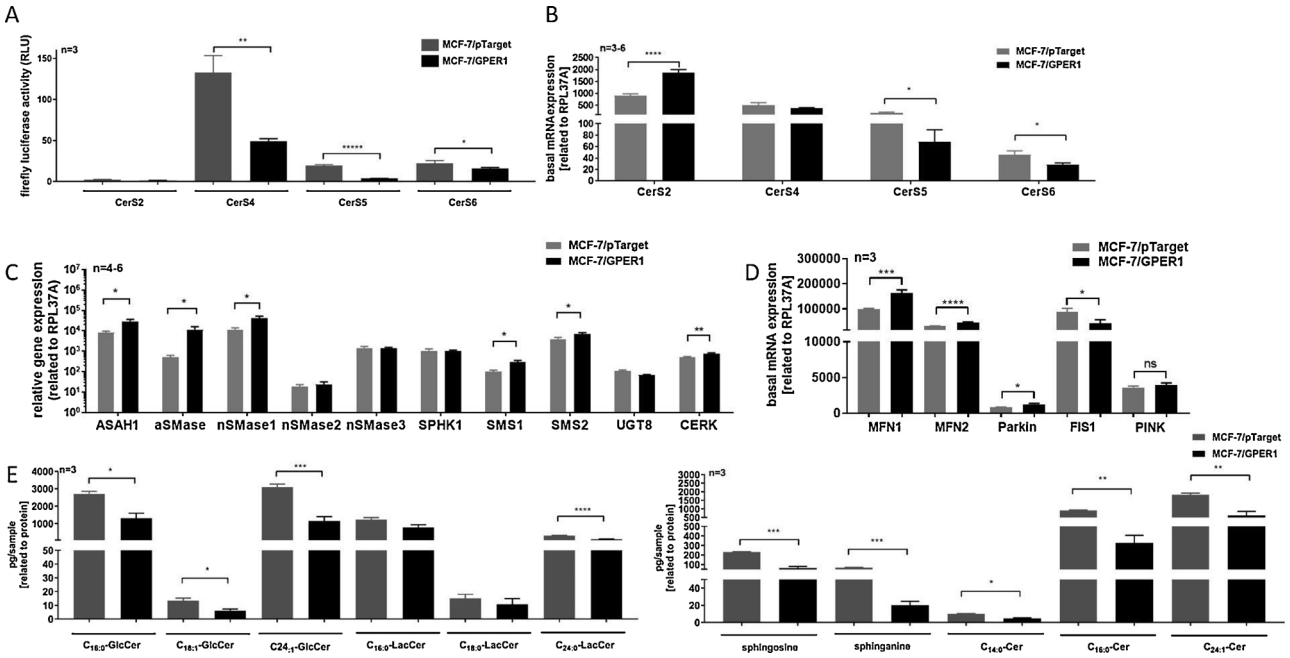

Fig. 6. GPER1 effect on CerS regulation in MCF-7/GPER1 cells. (A) MCF-7/pTarget and MCF-7/GPER1 cells were transfected with the CerS2, -4, -5 or -6 promoter plasmid and subsequently luciferase reporter gene assays performed. Data are represented as a mean of n = 3–5 ± SEM (standard error of the mean). Unpaired *t* test with Welch's correction. (B) CerS2, -4, -5 or -6 mRNA expression determination by qRT-PCR. The expression is related to the housekeeping gene RPL37A. Data are represented as a mean of n = 3–6 ± SEM (standard error of the mean). Unpaired *t* test with Welch's correction. (C) Sphingolipid enzyme mRNA expression determination by qRT-PCR. The expression is related to the housekeeping gene RPL37A. Data are represented as a mean of n = 4–6 ± SEM (standard error of the mean). Unpaired *t* test with Welch's correction. (D) In mitochondrial biogenesis involved protein mRNA expression determination by qRT-PCR. The expression is related to the housekeeping gene RPL37A. Data are represented as a mean of n = 3 ± SEM (standard error of the mean). Unpaired *t* test with Welch's correction. (*E*) Determination of sphingosine, sphinganine, $C_{14:0}$-, $C_{16:0}$-Cer, $C_{24:1}$-Cer $C_{16:0}$-GlcCer, $C_{18:1}$-GlcCer, $C_{24:1}$-GlcCer, $C_{16:0}$-LacCer, $C_{18:0}$-LacCer and $C_{24:0}$-LacCer levels by LC–MS/MS. Data are represented as a mean of n = 3 ± SEM (standard error of the mean). Unpaired *t* test with Welch's correction. $^{*}p \leq 0.05$, $^{**}p \leq 0.01$, $^{***}p \leq 0.001$, $^{****}p \leq 0.0001$.

Recently, Sun et al. showed that treatment with 17β-estradiol resulted in the expression of GPER1 and enhanced mitophagy through GPER1 and ERK1/2 signaling pathway in murine osteoblasts (Sun et al., 2018). However, a connection between increased expression of GPER1 and fewer mitophagosomes was found in chondrocytes (Fan et al., 2018) and GPER1 activation confers cardioprotective effects by protecting against mitophagy (Feng et al., 2017). The higher mitophagy activity could be the reason for the reduced ATP production and glycolytic capacity, but less mitochondrial mass could result in a pro-survival autophagy process as well. Reduction of FIS1 mRNA expression could be mediated by increased Parkin mRNA expression (Mai et al., 2010), which is in turn regulated by **PINK** activity. Since **PINK** mRNA is not more expressed following GPER1 overexpression, it is possible that the **PINK** activity is increased. Accumulated on the outer membrane of dysfunctional mitochondria, active **PINK** recruits Parkin (increased mRNA expression) to the mitochondria leading to autophagy (Fig. 8). This process promotes cell survival by removing dysfunctional mitochondria via mitophagy that might otherwise induce the process of apoptosis (reviewed in (Barodia et al., 2017)) and therefore protects cells from stress-induced apoptosis. Together, PINK and Parkin modify MFN1 and MFN2 (reviewed in (Truban et al., 2017)), which are both increased on mRNA expression level following GPER1 overexpression and promote mitochondrial fusion (Chen et al., 2003). The mitophagy, which might be the reason for the reduced ability to generate energy seems to affect the proliferation since MCF-7/GPER1 cells proliferate less than control cells. Therefore, we investigated the ability of colony formation of MCF-7/GPER1 and control cells under cyclophosphamide and doxorubicin stimulation.

Our data clearly show that GPER1 overexpression leads to a desensitization against doxorubicin. Besides MCF-7/GPER1 cells appears to induce mechanisms to reduce cyclophosphamide sensitivity. The reduced cell viability of MCF-7/GPER1 cells under cyclophosphamide treatment is not detectable in the 10 days ongoing colony forming assay meaning possible induction of multidrug resistance protein synthesis in GPER1 overexpressing cells. A decreased proliferation rate, which MCF-7/GPER1 cells exhibit, as well as the block of cell cycle in the G1 phase allows cells to elude of the cytotoxic effect of these compounds, which are mainly S phase dependent. Furthermore, a prolonged proliferation time enables cells to repair DNA-damage induced by drugs more effectively. This could be the reason for less doxorubicin sensitivity of MCF-7/GPER1 as compared to control cells. Furthermore, these mechanisms could be the reason why MCF-7/GPER1 cells develop a similar tolerance to cyclophosphamide as the control cells following 10 days of cultivation despite the reduced cell viability following 48 h treatment. Co-stimulation with fulvestrant sensitized both cell lines to doxorubicin, whereas only MCF-7/GPER1 cells are affected by cyclophosphamide and fulvestrant treatment. Cyclophosphamide is an alkylating agent leading to alkyl group attachment to the DNA, which results in DNA fragmentation by repair enzymes. In addition, the DNA is damaged by cross links and mispairing of nucleotides results in mutations, which occur following cyclophosphamide treatment (Khan and Middleton, 2007). Doxorubicin intercalates with the DNA as well, but leads also for example to the generation of free radicals, which impacts cell health (Thorn et al., 2011). If GPER1 overexpression impacts the cell radical elimination system, doxorubicin and cyclophosphamide could have different effects on MCF-7/GPER1 and control cells following fulvestrant treatment. The precise underlying mechanisms need to be investigated in the future. Recently, combination treatment with fulvestrant and doxorubicin showed synergistic effects and chemoresistance inducing factors such as Bcl2 and microtubule-associated protein tau were downregulated by fulvestrant (Huang et al., 2017). Dolfi et al. showed that fulvestrant sensitizes human breast cancer cells to

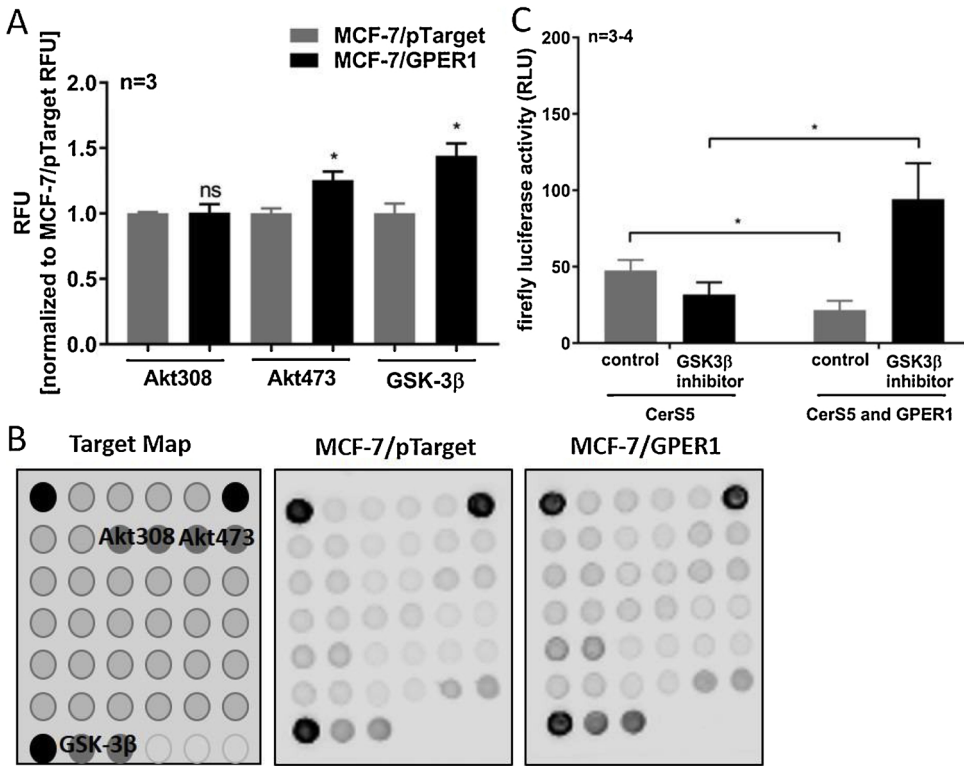

Fig. 7. GPER1 effect on GSK-3β activity and subsequently CerS5 promoter activity regulation. (A) Densitometrical analysis of an antibody-based array, which allows identification of phosphorylated signaling molecules. Data are represented as a mean of n = 3 ± SEM (standard error of the mean). Unpaired *t* test with Welch's correction. (B) Representative arrays were displayed. (C) Luciferase reporter gene assay following GPER1 and CerS5 promoter plasmid transfection and stimulation for 16 h with the GSK-3β inhibitor SB-216763. Data are represented as a mean of n = 3–4 ± SEM (standard error of the mean). Unpaired *t* test with Welch's correction. $*p \leq 0.05$.

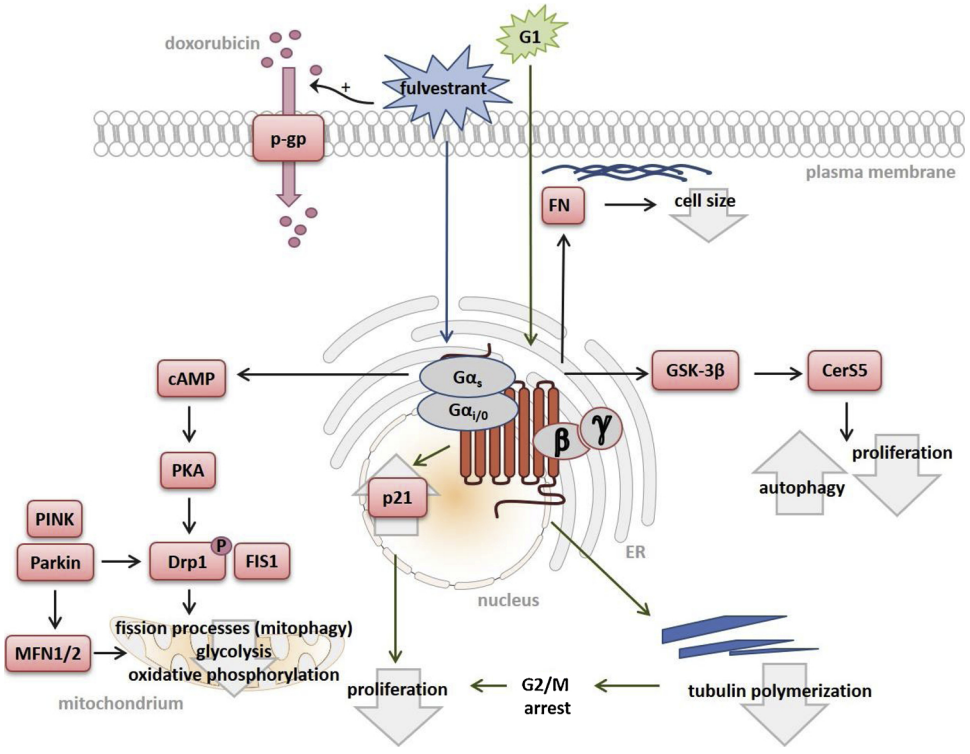

Fig. 8. Hypothesis of the GPER1 overexpression mediated effect and the impact of G1 and fulvestrant treatment. GPER1, localized in the ER and in perinuclear structures, leads to an increased cAMP concentration, presumably via the $G\alpha_s$ protein, which in turn activates PKA. PKA might deactivate Drp1 by phosphorylation. Drp1 together with FIS1 lead to increased fission events. Regulation of Drp1 and FIS1 could also be regulated by PINK and Parkin. PINK/Parkin might lead to increased MFN1/2 mRNA expression, which leads to increased fusion events in the mitochondria (mitophagy) resulting in reduced ability of energy production. In addition, GPER1 affects FN and other adhesion proteins resulting in a decreased cell size. GPER1 overexpression alters CerS expression, which leads to an induction of autophagy and a decreased proliferation. G1 treatment inhibits tubulin polymerization and induces p21 expression resulting in G2/M phase arrest and decreased proliferation. Fulvestrant treatment is followed by reinforcement of increased autophagy and decreased proliferation. Additionally, fulvestrant may interact with p-glycoprotein (p-gp), which leads to increased accumulation of doxorubicin in the cell. FN = fibronectin, PKA = protein kinase A, p-gp = P-glycoprotein, Drp1 = dynamin-related protein 1, P = phosphorylation, FIS1 = mitochondrial fission 1 protein, PINK = mitochondrial serine/threonine protein kinase, MFN1/2 = mitofusion 1/2, ER = endoplasmic reticulum.

chemotherapeutic drugs in MCF-7 and T47D cells (Dolfi et al., 2014). In ER - multidrug resistant cells fulvestrant leads to induced cytotoxicity, apoptosis and G2/M arrest. Furthermore, fulvestrant functions as a substrate of P-glycoprotein, which means that it competes with other drugs leading to an intracellular accumulation of for example doxorubicin (Huang et al., 2017). We could show that treatment of MCF-7/GPER1 cells with the GPER1 agonist G1 leads to a G2 phase arrest. G1 has been shown to block tubulin polymerization and thereby interrupt microtubule assembly in ovarian cancer cells leading to a G2/M phase arrest and suppression of ovarian cancer cell proliferation (Holm et al., 2011) (Fig. 8). G1 induces accumulation of cells in the S and G2 phases of the cell cycle by induction of p21 expression (Chan et al., 2010) (Fig. 8). However, in our cell system the G2 phase arrest after G1 treatment occurs independently of GPER1 overexpression.

Since sphingolipids control cell growth and proliferation, we investigated the expression of CerS and other sphingolipid metabolizing enzymes. Previously, we reported that GPER1 overexpression influences CerS promoter activity (Wegner et al., 2014). In this study we detected a decrease of CerS mRNA expression. Expression of aSMase/nSMase1 and SMS1/SMS2, ASAH1 and CERK mRNA is also increased. Studies revealed a link between increased ASAH1 expression and a better prognosis in ER + breast cancer (Ruckhäberle et al., 2009), whereas upregulation of CERK after HER2 inhibition was associated with an increased risk of recurrence in breast cancer patients (Payne et al., 2014). The sphingomyelin content in cells is strictly regulated by sphingomyelinases and sphingomyelin synthases, which activities create a balance between sphingomyelin synthesis and degradation. Sphingomyelin is an important modulator of membrane properties and involved in cellular proliferation, growth and apoptosis (reviewed in (Jenkins et al., 2009; Kolesnick, 1991; Levade and Jaffrezou, 1999)). Hartmann et al. demonstrated that upregulation of CerS4 and CerS6 leads to inhibition of cell proliferation and induction of apoptosis, whereas upregulated CerS2 increases proliferation (Hartmann et al., 2012). Overexpression of CerS6 sensitized cisplatin resistant cells (Cal27-CisR cells) to cisplatin via CerS6-mediated activation of calpain, a Ca^{2+}-dependent cysteine protease, which inhibits autophagy, while cisplatin resistance was associated with a low CerS6 expression and enhanced protective autophagy (Li et al., 2018). CerS5 was recently associated with protective autophagy (Fitzgerald et al., 2015). The study shows that modulation of autophagy by CerS5/6 and C16-dihydroceramide/-ceramide contributes to chemosensitivity of various cancer cells.

Following GPER1 overexpression increased levels of Akt473 and unaltered Akt308 levels were detected. This indicates that GSK-3β is not inhibited by Akt308, which is a known regulatory mechanism (reviewed in (Zhang et al., 2017)). Accordingly, the GSK-3β is activated by phosphorylation, which is known to be mediated by phosphorylation at Tyr279/216 (reviewed in (Grimes and Jope, 2001; Liang and Chuang, 2007; Krishnankutty et al., 2017)). How GSK-3β regulates CerS5 promoter activity exactly (Fig. 8), needs to be investigated in future studies.

5. Conclusion

In conclusion, GPER1 overexpression leads to inhibition of cell proliferation in human ER + breast cancer cells, which was accompanied by a cell cycle arrest, autophagy induction and reduced mitochondrial activity (mitophagy). These effects might be mediated by reduced CerS5 synthesis, which is regulated by GSK-3β. In addition, cytostatic drug resistance, possibly as a consequence of reduced proliferation of MCF-7/GPER1, could be reversed by the SERD fulvestrant.

Declarations of interest

None.

Acknowledgements

This work was supported by the Deutsche Forschungsgemeinschaft (WE 5825/1-1), the August Scheidel-Stiftung, the Heinrich und Fritz Riese-Stiftung (Die Rolle der Ceramidsynthasen 2 4 5 und 6 als Transkriptionsfaktoren und Identifizierung der von ihnen regulierten und in pathophysiologischen Prozessen involvierten Proteine), the Paul und Ursula Klein-Stiftung (Identifizierung von Sphingolipid-abhängig regulierten Membranproteinen in Brust und Darmkrebszellen) and the Johanna Quandt-Jubiläumsfond (UDP-Glukose Ceramidglykosyltransferase (UGCG)-induzierte hepatische Tumorentstehung).

Appendix A. Supplementary data

Supplementary material related to this article can be found, in the online version, at doi:https://doi.org/10.1016/j.biocel.2019.05.002.

References

Ferlay, J., Soerjomataram, I., Dikshit, R., Eser, S., Mathers, C., Rebelo, M., Parkin, D.M., Forman, D., Bray, F., 2015. Cancer incidence and mortality worldwide: sources, methods and major patterns in GLOBOCAN 2012. Int. J. Cancer 136, E359–86.

Pujol, P., Hilsenbeck, S.G., Chamness, G.C., Elledge, R.M., 1994. Rising levels of estrogen receptor in breast cancer over 2 decades. Cancer 74, 1601–1606.

Chu, K.C., Anderson, W.F., 2002. Rates for breast cancer characteristics by estrogen and progesterone receptor status in the major racial/ethnic groups. Breast Cancer Res. Treat. 74 (Jun), 199–211.

Carmeci, C., Thompson, D.A., Ring, H.Z., Francke, U., Weigel, R.J., 1997. Identification of a gene (GPR30) with homology to the G-protein-coupled receptor superfamily associated with estrogen receptor expression in breast cancer. Genomics 45 (Nov), 607–617.

Olde, B., Leeb-Lundberg, L.M.F., 2009. GPR30/GPER1: searching for a role in estrogen physiology. Trends Endocrinol. Metab. 20, 409–416. https://doi.org/10.1016/j.tem.2009.04.006.

Wang, D., Hu, L., Zhang, G., Zhang, L., Chen, C., 2010. G protein-coupled receptor 30 in tumor development. Endocrine 38, 29–37. https://doi.org/10.1007/s12020-010-9363-z.

Vivacqua, A., Romeo, E., Marco, P., Francesco, E.M., Abonante, S., Maggiolini, M., 2012. GPER mediates the Egr-1 expression induced by 17beta-estradiol and 4-hydroxitamoxifen in breast and endometrial cancer cells. Breast Cancer Res. Treat. 133, 1025–1035.

Pupo, M., Pisano, A., Lappano, R., Santolla, M.F., Francesco, E.M., Abonante, S., Rosano, C., Maggiolini, M., 2012. Bisphenol A induces gene expression changes and proliferative effects through GPER in breast cancer cells and cancer-associated fibroblasts. Environ. Health Perspect. 120, 1177–1182.

Filardo, E.J., Quinn, J.A., Sabo, E., 2008. Association of the membrane estrogen receptor, GPR30, with breast tumor metastasis and transactivation of the epidermal growth factor receptor. Steroids 73, 870–873. https://doi.org/10.1016/j.steroids.2007.12.025.

Ignatov, A., Ignatov, T., Roessner, A., Costa, S.D., Kalinski, T., 2010. Role of GPR30 in the mechanisms of tamoxifen resistance in breast cancer MCF-7 cells. Breast Cancer Res. Treat. 123, 87–96. https://doi.org/10.1007/s10549-009-0624-6.

Ignatov, A., Ignatov, T., Weissenborn, C., Eggemann, H., Bischoff, J., Semczuk, A., Roessner, A., Costa, S.D., Kalinski, T., 2011. G-protein-coupled estrogen receptor GPR30 and tamoxifen resistance in breast cancer. Breast Cancer Res. Treat. 128, 457–466. https://doi.org/10.1007/s10549-011-1584-1.

Giessrigl, B., Schmidt, W.M., Kalipciyan, M., Jeitler, M., Bilban, M., Gollinger, M., Krieger, S., Jäger, W., Mader, R.M., Krupitza, G., 2013. Fulvestrant induces resistance by modulating GPER and CDK6 expression: implication of methyltransferases, deacetylases and the hSWI/SNF chromatin remodelling complex. Br. J. Cancer 109, 2751–2762. https://doi.org/10.1038/bjc.2013.583.

Prossnitz, E.R., Arterburn, J.B., Smith, H.O., Oprea, T.I., Sklar, L.A., Hathaway, H.J., 2008. Estrogen signaling through the transmembrane G protein-coupled receptor GPR30. Annu. Rev. Physiol. 70, 165–190. https://doi.org/10.1146/annurev.physiol.70.113006.100518.

Nilsson, B.-O., Olde, B., Leeb-Lundberg, L.M.F., 2011. G protein-coupled oestrogen receptor 1 (GPER1)/GPR30: a new player in cardiovascular and metabolic oestrogenic signalling. Br. J. Pharmacol. 163, 1131–1139. https://doi.org/10.1111/j.1476-5381.2011.01235.x.

Maggiolini, M., Vivacqua, A., Fasanella, G., Recchia, A.G., Sisci, D., Pezzi, V., Montanaro, D., Musti, A.M., Picard, D., Andò, S., 2004. The G protein-coupled receptor GPR30 mediates c-fos up-regulation by 17beta-estradiol and phytoestrogens in breast cancer cells. J. Biol. Chem. 279, 27008–27016. https://doi.org/10.1074/jbc.M403588200.

Ariazi, E.A., Brailoiu, E., Yerrum, S., Shupp, H.A., Slifker, M.J., Cunliffe, H.E., Black, M.A., Donato, A.L., Arterburn, J.B., Oprea, T.I., et al., 2010. The G Protein–coupled receptor GPR30 inhibits proliferation of estrogen receptor–positive breast cancer cells. Cancer Res. 70, 1184–1194. https://doi.org/10.1158/0008-5472.CAN-09-3068.

Wegner, M.-S., Wanger, R.A., Oertel, S., Brachtendorf, S., Hartmann, D., Schiffmann, S., Marschalek, R., Schreiber, Y., Ferreirós, N., Geisslinger, G., et al., 2014. Ceramide synthases CerS4 and CerS5 are upregulated by 17β-estradiol and GPER1 via AP-1 in

human breast cancer cells. Biochem. Pharmacol. 92, 577–589. https://doi.org/10.1016/j.bcp.2014.10.007.
Wegner, M.-S., Schiffmann, S., Parnham, M.J., Geisslinger, G., Grösch, S., 2016. The enigma of ceramide synthase regulation in mammalian cells. Prog. Lipid Res. 63, 93–119. https://doi.org/10.1016/j.plipres.2016.03.006.
Yamane, M., Miyazawa, K., Moriya, S., Abe, A., Yamane, S.D., 2011. L-Threo-1-phenyl-2-decanoylamino-3-morpholino-1-propanol (DL-PDMP) increases endoplasmic reticulum stress, autophagy and apoptosis accompanying ceramide accumulation via ceramide synthase 5 protein expression in A549 cells. Biochimie 93, 1446–1459. https://doi.org/10.1016/j.biochi.2011.04.016.
Fitzgerald, S., Sheehan, K.M., Espina, V., O'Grady, A., Cummins, R., Kenny, D., Liotta, L., O'Kennedy, R., Kay, E.W., Kijanka, G.S., 2015. High CerS5 expression levels associate with reduced patient survival and transition from apoptotic to autophagy signalling pathways in colorectal cancer. J. Pathol. Clin. Res. 1, 54–65. https://doi.org/10.1002/cjp2.5.
Brachtendorf, S., Wanger, R.A., Birod, K., Thomas, D., Trautmann, S., Wegner, M.-S., Fuhrmann, D.C., Brüne, B., Geisslinger, G., Grösch, S., 2018. Chemosensitivity of human colon cancer cells is influenced by a p53-dependent enhancement of ceramide synthase 5 and induction of autophagy. Biochim. Biophys. Acta (BBA) 1863, 1214–1227. https://doi.org/10.1016/j.bbalip.2018.07.011.
Oo, P.S., Yamaguchi, Y., Sawaguchi, A., Tin Htwe Kyaw, M., Choijookhuu, N., Noor Ali, M., Srisowanna, N., Hino, S.-i., Hishikawa, Y., 2018. Estrogen regulates mitochondrial morphology through phosphorylation of dynamin-related protein 1 in MCF7 human breast Cancer cells. Acta Histochem. Cytochem. 51, 21–31. https://doi.org/10.1267/ahc.17034.
Klinge, C.M., 2017. Estrogens regulate life and death in mitochondria. J. Bioenergy Biomembr. 49, 307–324. https://doi.org/10.1007/s10863-017-9704-1.
Bjørkøy, G., Lamark, T., Brech, A., Outzen, H., Perander, M., Overvatn, A., Stenmark, H., Johansen, T., 2005. p62/SQSTM1 forms protein aggregates degraded by autophagy and has a protective effect on huntingtin-induced cell death. J. Cell Biol. 171, 603–614. https://doi.org/10.1083/jcb.200507002.
Grösch, S., Schiffmann, S., Geisslinger, G., 2012. Chain length-specific properties of ceramides. Prog. Lipid Res. 51, 50–62. https://doi.org/10.1016/j.plipres.2011.11.001.
Broselid, S., Cheng, B., Sjostrom, M., Lovgren, K., Klug-De Santiago, H.L.P., Belting, M., Jirstrom, K., Malmstrom, P., Olde, B., Bendahl, P.-O., et al., 2013. G protein-coupled estrogen receptor is apoptotic and correlates with increased distant disease-free survival of estrogen receptor-positive breast cancer patients. Clin. Cancer Res. 19, 1681–1692. https://doi.org/10.1158/1078-0432.CCR-12-2376.
Jiang, Q.-F., Wu, T.-T., Yang, J.-Y., Dong, C.-R., Wang, N., Liu, X.-H., Liu, Z.-M., 2013. 17β-Estradiol promotes the invasion and migration of nuclear estrogen receptor-negative breast cancer cells through cross-talk between GPER1 and CXCR1. J. Steroid Biochem. Mol. Biol. 138, 314–324. https://doi.org/10.1016/j.jsbmb.2013.07.011.
Yang, F., Shao, Z.-M., 2016. Double-edged role of G protein-coupled estrogen receptor 1 in breast cancer prognosis: an analysis of 167 breast cancer samples and online data sets. OTT 9, 6407–6415. https://doi.org/10.2147/OTT.S111846.
Revankar, C.M., 2005. A transmembrane intracellular estrogen receptor mediates rapid cell signaling. Science (80-) 307, 1625–1630. https://doi.org/10.1126/science.1106943.
Pupo, M., Bodmer, A., Berto, M., Maggiolini, M., Dietrich, P.-Y., Picard, D., 2017. A genetic polymorphism repurposes the G-protein coupled and membrane-associated estrogen receptor GPER to a transcription factor-like molecule promoting paracrine signaling between stroma and breast carcinoma cells. Oncotarget 8. https://doi.org/10.18632/oncotarget.18156.
Quinn, J.A., Graeber, C.T., Frackelton, A.R., Kim, M., Schwarzbauer, J.E., Filardo, E.J., 2009. Coordinate regulation of estrogen-mediated fibronectin matrix assembly and epidermal growth factor receptor transactivation by the G Protein-coupled receptor, GPR30. Mol. Endocrinol. 23, 1052–1064. https://doi.org/10.1210/me.2008-0262.
Magruder, H.T., Quinn, J.A., Schwartzbauer, J.E., Reichner, J., Huang, A., Filardo, E.J., 2014. The G protein-coupled estrogen receptor-1, GPER-1, promotes fibrillogenesis via a Shc-dependent pathway resulting in anchorage-independent growth. Horm. Cancer 5, 390–404. https://doi.org/10.1007/s12672-014-0195-9.
Kang, N., Shah, V.H., Urrutia, R., 2015. Membrane-to-nucleus signals and epigenetic mechanisms for myofibroblastic activation and desmoplastic stroma: potential therapeutic targets for liver metastasis? Mol. Cancer Res. MCR 13, 604–612.
Hu, C., Huang, Y., Li, L., 2017. Drp1-dependent mitochondrial fission plays critical roles in physiological and pathological progresses in mammals. Int. J. Mol. Sci. 18. https://doi.org/10.3390/ijms18010144.
Mozdy, A.D., McCaffery, J.M., Shaw, J.M., 2000. Dnm1p GTPase-mediated mitochondrial fission is a multi-step process requiring the novel integral membrane component Fis1p. J. Cell Biol. 151, 367–380.
Jahani-Asl, A., Slack, R.S., 2007. The phosphorylation state of Drp1 determines cell fate. EMBO Rep. 8, 912–913. https://doi.org/10.1038/sj.embor.7401077.
Youle, R.J., van der Bliek, A.M., 2012. Mitochondrial fission, fusion, and stress. Science 337, 1062–1065. https://doi.org/10.1126/science.1219855.
Sun, X., Yang, X., Zhao, Y., Li, Y., Guo, L., 2018. Effects of 17β-Estradiol on mitophagy in the murine MC3T3-E1 osteoblast cell line is mediated via g protein-coupled estrogen receptor and the ERK1/2 signaling pathway. Med. Sci. Monit. 24, 903–911. https://doi.org/10.12659/MSM.908705.
Fan, D.-x., Yang, X.-h., Li, Y.-n., Guo, L., 2018. 17β-estradiol on the expression of G-Protein coupled estrogen receptor (GPER/GPR30) mitophagy, and the PI3K/Akt signaling pathway in ATDC5 chondrocytes in vitro. Med. Sci. Monit. 24, 1936–1947. https://doi.org/10.12659/MSM.909365.
Feng, Y., Madungwe, N.B., da Cruz Junho, C.V., Bopassa, J.C., 2017. Activation of G protein-coupled oestrogen receptor 1 at the onset of reperfusion protects the myocardium against ischemia/reperfusion injury by reducing mitochondrial dysfunction and mitophagy. Br. J. Pharmacol. 174, 4329–4344. https://doi.org/10.1111/bph.14033.
Mai, S., Klinkenberg, M., Auburger, G., Bereiter-Hahn, J., Jendrach, M., 2010. Decreased expression of Drp1 and Fis1 mediates mitochondrial elongation in senescent cells and enhances resistance to oxidative stress through PINK1. J. Cell. Sci. 123, 917–926. https://doi.org/10.1242/jcs.059246.
Barodia, S.K., Creed, R.B., Goldberg, M.S., 2017. Parkin and PINK1 functions in oxidative stress and neurodegeneration. Brain Res. Bull. 133, 51–59. https://doi.org/10.1016/j.brainresbull.2016.12.004.
Truban, D., Hou, X., Caulfield, T.R., Fiesel, F.C., Springer, W., 2017. PINK1, Parkin, and mitochondrial quality control: what can we learn about Parkinson's disease pathobiology? J. Parkinsons Dis. 7, 13–29. https://doi.org/10.3233/JPD-160989.
Chen, H., Detmer, S.A., Ewald, A.J., Griffin, E.E., Fraser, S.E., Chan, D.C., 2003. Mitofusins Mfn1 and Mfn2 coordinately regulate mitochondrial fusion and are essential for embryonic development. J. Cell Biol. 160, 189–200. https://doi.org/10.1083/jcb.200211046.
Khan, O., Middleton, M.R., 2007. The therapeutic potential of O6-alkylguanine DNA alkyltransferase inhibitors. Expert Opin. Investig. Drugs 16, 1573–1584. https://doi.org/10.1517/13543784.16.10.1573.
Thorn, C.F., Oshiro, C., Marsh, S., Hernandez-Boussard, T., McLeod, H., Klein, T.E., Altman, R.B., 2011. Doxorubicin pathways: pharmacodynamics and adverse effects. Pharmacogenet. Genomics 21, 440–446. https://doi.org/10.1097/FPC.0b013e32833ffb56.
Huang, Y., Jiang, D., Sui, M., Wang, X., Fan, W., 2017. Fulvestrant reverses doxorubicin resistance in multidrug-resistant breast cell lines independent of estrogen receptor expression. Oncol. Rep. 37, 705–712.
Dolfi, S.C., Jäger, A.V., Medina, D.J., Haffty, B.G., Yang, J.-M., Hirshfield, K.M., 2014. Fulvestrant treatment alters MDM2 protein turnover and sensitivity of human breast carcinoma cells to chemotherapeutic drugs. Cancer Lett. 350, 52–60. https://doi.org/10.1016/j.canlet.2014.04.009.
Holm, A., Baldetorp, B., Olde, B., Leeb-Lundberg, L.M.F., Nilsson, B.-O., 2011. The GPER1 agonist G-1 attenuates endothelial cell proliferation by inhibiting DNA synthesis and accumulating cells in the S and G2 phases of the cell cycle. J. Vasc. Res. 48, 327–335. https://doi.org/10.1159/000322578.
Chan, Q.K.Y., Lam, H.-M., Ng, C.-F., Lee, A.Y.Y., Chan, E.S.Y., Ng, H.-K., Ho, S.-M., Lau, K.-M., 2010. Activation of GPR30 inhibits the growth of prostate cancer cells through sustained activation of Erk1/2, c-jun/c-fos-dependent upregulation of p21, and induction of G(2) cell-cycle arrest. Cell Death Differ. 17, 1511–1523. https://doi.org/10.1038/cdd.2010.20.
Ruckhäberle, E., Holtrich, U., Engels, K., Hanker, L., Gätje, R., Metzler, D., Karn, T., Kaufmann, M., Rody, A., 2009. Acid ceramidase 1 expression correlates with a better prognosis in ER-positive breast cancer. DCLI 12, 502–513. https://doi.org/10.3109/13697130902939913.
Payne, A.W., Pant, D.K., Pan, T.-C., Chodosh, L.A., 2014. Ceramide kinase promotes tumor cell survival and mammary tumor recurrence. Cancer Res. 74, 6352–6363. https://doi.org/10.1158/0008-5472.CAN-14-1292.
Jenkins, R.W., Canals, D., Hannun, Y.A., 2009. Roles and regulation of secretory and lysosomal acid sphingomyelinase. Cell. Signal. 21, 836–846.
Kolesnick, R.N., 1991. Sphingomyelin and derivatives as cellular signals. Prog. Lipid Res. 30, 1–38.
Levade, T., Jaffrezou, J.-P., 1999. Signalling sphingomyelinases: Which, where, how and why? Biochim. Biophys. Acta 1438, 1–17.
Hartmann, D., Lucks, J., Fuchs, S., Schiffmann, S., Schreiber, Y., Ferreirós, N., Merkens, J., Marschalek, R., Geisslinger, G., Grösch, S., 2012. Long chain ceramides and very long chain ceramides have opposite effects on human breast and colon cancer cell growth. Int. J. Biochem. Cell Biol. 44, 620–628. https://doi.org/10.1016/j.biocel.2011.12.019.
Li, S., Wu, Y., Ding, Y., Yu, M., Ai, Z., 2018. CerS6 regulates cisplatin resistance in oral squamous cell carcinoma by altering mitochondrial fission and autophagy. J. Cell. Physiol. 233, 9416–9425. https://doi.org/10.1002/jcp.26815.
Zhang, Z., Liu, H., Liu, J., 2017. Akt activation: a potential strategy to ameliorate insulin resistance. Diabetes Res. Clin. Pract. https://doi.org/10.1016/j.diabres.2017.10.004.
Grimes, C.A., Jope, R.S., 2001. The multifaceted roles of glycogen synthase kinase 3beta in cellular signaling. Prog. Neurobiol. 65, 391–426.
Liang, M.-H., Chuang, D.-M., 2007. Regulation and function of glycogen synthase kinase-3 isoforms in neuronal survival. J. Biol. Chem. 282, 3904–3917. https://doi.org/10.1074/jbc.M605178200.
Krishnankutty, A., Kimura, T., Saito, T., Aoyagi, K., Asada, A., Takahashi, S.-I., Ando, K., Ohara-Imaizumi, M., Ishiguro, K., Hisanaga, S.-i., 2017. In vivo regulation of glycogen synthase kinase 3β activity in neurons and brains. Sci. Rep. 7. https://doi.org/10.1038/s41598-017-09239-5.